Australasian impact crater buried under the Bolaven volcanic field, Southern Laos

Kerry Sieh[a,1], Jason Herrin[a], Brian Jicha[b], Dayana Schonwalder Angel[a], James D. P. Moore[a], Paramesh Banerjee[a], Weerachat Wiwegwin[c], Vanpheng Sihavong[d], Brad Singer[b], Tawachai Chualaowanich[c], and Punya Charusiri[e]

[a]Earth Observatory of Singapore, Nanyang Technological University, 639798 Singapore; [b]Department of Geoscience, University of Wisconsin–Madison, Madison, WI 53706; [c]Department of Mineral Resources, Ministry of Natural Resources and Environment, Ratchatewi, 10400 Bangkok, Thailand; [d]Department of Geology and Mines, Ministry of Energy and Mines, Vientiane, Lao People's Democratic Republic; and [e]Department of Geology, Chulalongkorn University, Khet Pathumwan, 10330 Bangkok, Thailand

Contributed by Kerry Sieh, October 7, 2019 (sent for review March 13, 2019; reviewed by Fred Jourdan, Henry Jay Melosh, and John Douglas Yule)

The crater and proximal effects of the largest known young meteorite impact on Earth have eluded discovery for nearly a century. We present 4 lines of evidence that the 0.79-Ma impact crater of the Australasian tektites lies buried beneath lavas of a long-lived, 910-km^3 volcanic field in Southern Laos: 1) Tektite geochemistry implies the presence of young, weathered basalts at the site at the time of the impact. 2) Geologic mapping and ^{40}Ar-^{39}Ar dates confirm that both pre- and postimpact basaltic lavas exist at the proposed impact site and that postimpact basalts wholly cover it. 3) A gravity anomaly there may also reflect the presence of a buried ∼17 × 13-km crater. 4) The nature of an outcrop of thick, crudely layered, bouldery sandstone and mudstone breccia 10–20 km from the center of the impact and fractured quartz grains within its boulder clasts support its being part of the proximal ejecta blanket.

Australasian | impact | crater | Lao | tektite

The Australasian strewn field, a horizon of glassy clasts ("tektites") quenched from molten ejecta of a bolide impact about 0.79 Ma (1, 2), extends across about 1/10 of the Earth's surface (3)—from Indochina to East Antarctica and from the Indian to western Pacific Oceans (Fig. 1, *Inset*). The northwestward increase in both the abundance and the size of tektite specimens points to the impact site being in eastern central Indochina (3–7). This is within the region of Muong Nong-type tektites, the least streamlined, most volatile-rich, most siliceous, and largest of the ejected melt fragments. Their high silica content, relict grains, and other chemical characteristics indicate primarily quartz-rich coarse siltstone to fine sandstone target rocks (6, 8–10), perhaps of Jurassic age (11).

The Mystery of the Impact Site

Concentrations of microtektites and iridium in contemporaneous marine sediments more than a 1,000 km away from the impact region yield very poorly constrained estimates of crater diameter, ranging from 15 to 300 km (6, 7, 12–14). Given these large crater sizes, it is remarkable that the many searches of the past half-century have yielded neither a definitive impact site nor a proximal ejecta blanket (3, 4, 15–21). This failure implies either that a crater never formed (22, 23) or that either burial or erosion has obscured it.

The most promising place to look for either an eroded or a buried crater is within the largest, contiguous expanse of fine-grained, siliclastic Mesozoic sedimentary rocks in the region, the Khorat Plateau (Fig. 1). However, obscuration by erosion within this 155,000-km^2 region of predominantly gentle topography is not plausible. The crater rim is likely to have risen more than 100 m above the target surface (24), but postimpact erosion of the region by the Mekong River and its tributaries has been far less than this. This is clear from the facts that tektites occur in situ primarily on gentle surfaces no more than a few 10s of meters above modern nearby streams and that preimpact basalt flows cover surfaces that are only about 50 m above the streambed of the modern Mekong River (*SI Appendix*, Fig. S1 and Tektites Information_Dataset S1) (25).

Moreover, field examinations of candidates for an eroded crater—several large, circular, low-relief features in central Laos and northern Cambodia—have shown that these are, instead, eroded synclines in Mesozoic rocks (19). Likewise, our examination of a proposed crater in NE Cambodia (26) revealed that it is, in fact, the top of a granitoid pluton surrounded by a resistant contact-metamorphic quartzite aureole derived from surrounding Mesozoic sandstone. Another candidate crater in southern China appears to have a similar origin (27).

Burial of the impact crater might also seem unlikely, because adequately wide and thick postimpact sedimentation is nearly absent on the Khorat Plateau. The only notable exception is an extensive basaltic volcanic field centered on the Bolaven Plateau in Southern Laos (Fig. 1). We present evidence below that this thick pile of volcanic rocks does indeed bury the site of the impact.

The 6,000-km^2 Bolaven Plateau rises about 1 km above the Khorat Plateau in Southern Laos, east of the Mekong River (Fig. 2 and *SI Appendix*, Fig. S2). Fine-grained, nearly flat-lying Mesozoic quartz sandstones and mudstones underlie this elevated surface and crop out almost continuously around its cliffy perimeter (28). Judging from the nearly vertical pitches at the top

Significance

A field of black glassy blobs, strewn across about 20% of Earth's Eastern Hemisphere, resulted from the impact of a large meteorite about 790,000 y ago. The large crater from which these tektites originated has eluded discovery for over a century, although evidence has long pointed to a location somewhere within Indochina, near the northern limit of the strewn field. We present stratigraphic, geochemical, geophysical, and geochronological evidence that the ∼15-km diameter crater lies buried beneath a large, young volcanic field in Southern Laos.

Author contributions: K.S., J.H., D.S.A., J.D.P.M., and P.B. designed research; K.S., J.H., B.J., D.S.A., J.D.P.M., P.B., W.W., V.S., B.S., T.C., and P.C. performed research; K.S., J.H., B.J., D.S.A., J.D.P.M., P.B., B.S., and T.C. analyzed data; and K.S., J.H., B.J., D.S.A., J.D.P.M., P.B., and B.S. wrote the paper.

Reviewers: F.J., Curtin University; H.J.M., Purdue University; and J.D.Y., California State University, Northridge.

The authors declare no competing interest.

Data deposition: Supplementary datasets have been deposited in the public data repository hosted by Nanyang Technological University (DR-NTU), https://researchdata.ntu.edu.sg/ (DOI: 10.21979/N9/CTNDZQ).

See online for related content such as Commentaries.

[1]To whom correspondence may be addressed. Email: sieh@ntu.edu.sg.

This article contains supporting information online at https://www.pnas.org/lookup/suppl/doi:10.1073/pnas.1904368116/-/DCSupplemental.

First published December 30, 2019.

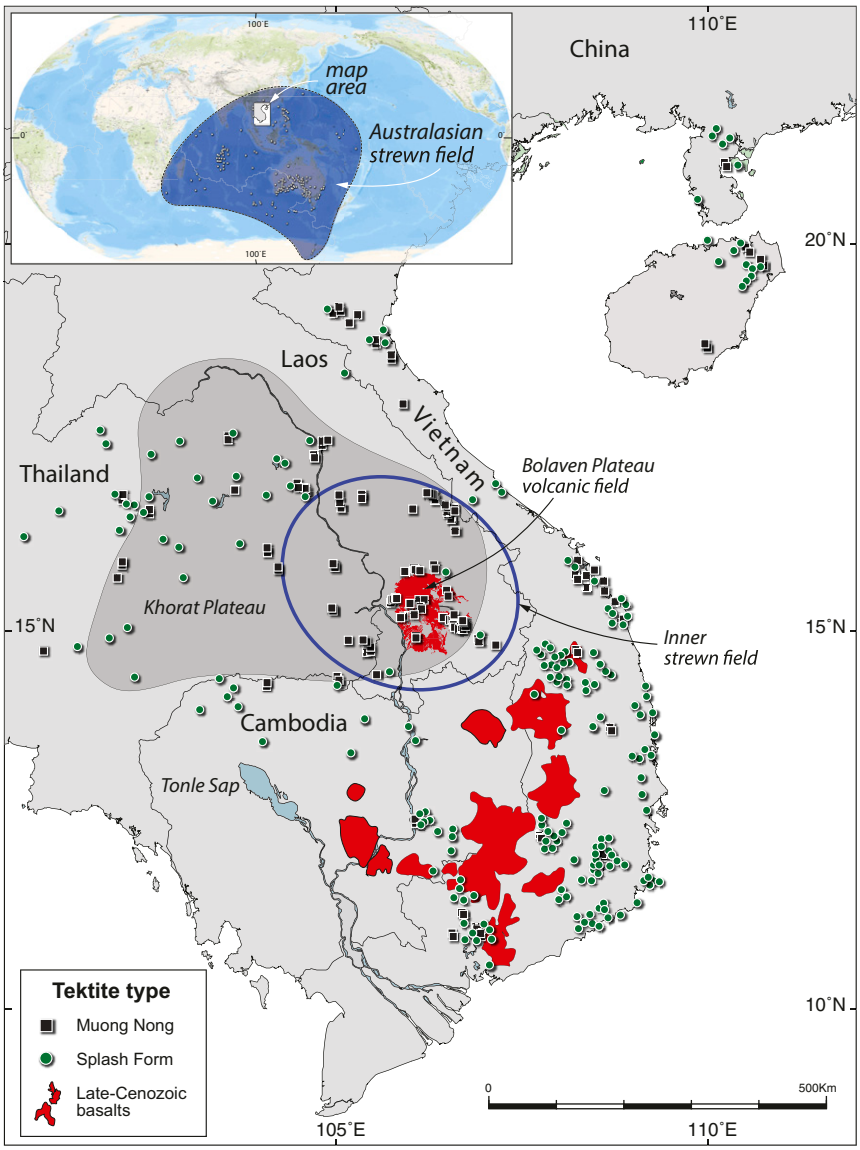

Fig. 1. The Bolaven Plateau volcanic field likely buries the impact crater that produced the tektites of the Australasian strewn field. It is the only adequately large and thick postimpact deposit on the Khorat Plateau, the largest region of plausible target rocks. It is also the only thick, postimpact deposit within the inner Muong Nong strewn field, the region containing exclusively nonaerodynamically shaped Muong-Nong–type tektites (circumscribed by the blue ellipse). Tektite find locations data from ref. 52 and this study. Basalt fields adapted with permission of ref. 53 and ref. 54; permission conveyed through Copyright Clearance Center, Inc. Outline of the Khorat Plateau data from ref. 55. *Inset*, finds of Australasian tektites and microtektites data from ref. 56 (white dots) define an asymmetric strewn field (blue).

of this perimeter cliff and from outcrops on the plateau, the uppermost 200–250 m of the Mesozoic bedrock comprise massive to cross-bedded fluvial sandstones. Gentler slopes below indicate that friable mudstones dominate the underlying 250 m. If the Australasian bolide struck the Bolaven Plateau, this 500-m-thick sandstone–mudstone sequence would have comprised much of the impacted target rock.

However, a basaltic volcanic field that covers an area of ~5,000 km^2 caps these rocks and spills down the flanks of the plateau. Structure contours drawn on the Mesozoic bedrock/basalt contact by interpolating under the lavas between bedrock outcrops allow us to create an isopach map of the volcanic field (*SI Appendix*, Fig. S3). From this we calculate a volcanic volume of ~910 km^3. In the vicinity of the summit region of the volcanic field, the basalt is up to ~300 m thick. This extent and thickness are great enough to hide a crater up to ~15 km in diameter and with a rim that rises up to a couple hundred meters above the bedrock surface.

Methodology: 4 Tests of the Hypothesis

We offer 4 tests of the hypothesis that the Australasian impact crater lies buried beneath the basaltic lavas of the Bolaven Plateau. First, we examine published geochemical analyses of the tektites to test whether or not they could include a basaltic component. If the bolide that created the Australasian tektites impacted a location that had a cover of mafic lavas, then the Bolaven volcanic field would be a prime candidate for the impact site. Second, we use the ^{40}Ar-^{39}Ar method to date many of the flows comprising the volcanic field, to see if they both antedate and postdate the impact. The presence of basalts older than the impact date would imply a contribution to the ejected materials. Basalts younger than the impact would need to wholly mantle the proposed impact site. Third, we conduct a field

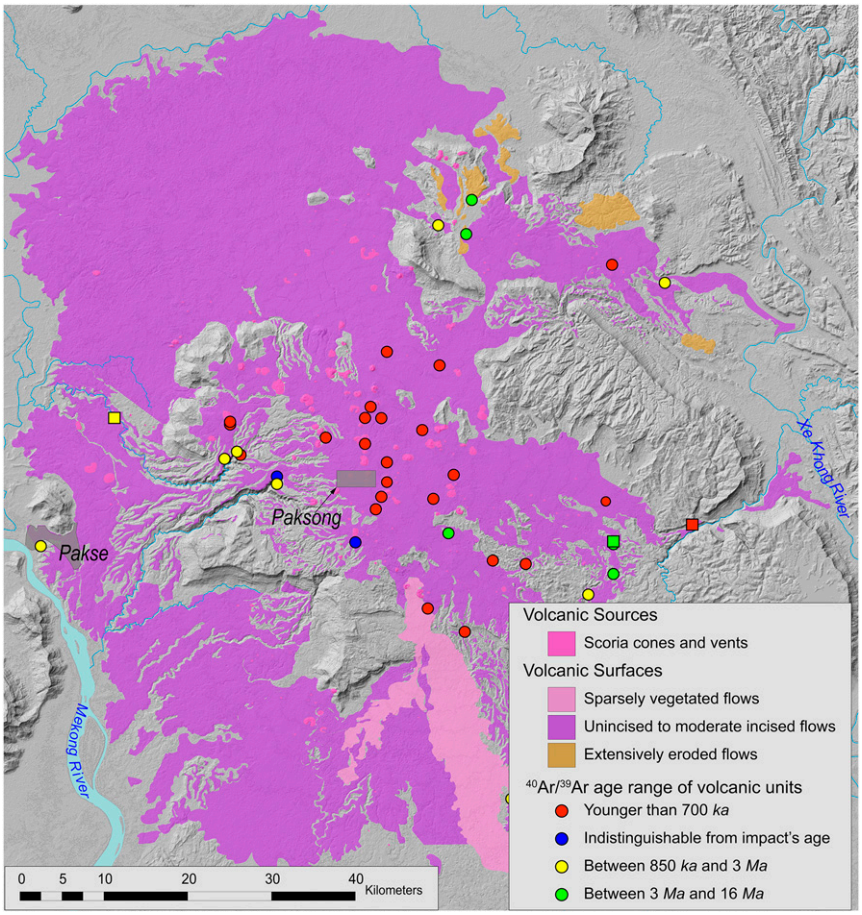

Fig. 2. The Bolaven volcanic field covers much of the Bolaven Plateau and spills over its kilometer-high flanks to the floodplain of the Mekong River. The perimeter cliffs of the plateau expose nearly flat-lying Mesozoic sandstones and mudstones like those inferred from tektite composition to be the dominant target rocks of the Australasian impactor. ^{40}Ar-^{39}Ar ages on lavas appear as dots colored according to age. Squares are previously published ages (35). See *SI Appendix*, Table S1 and Ar-Ar Metadata_Dataset S3 (25) for details on geochronology and *SI Appendix*, Fig. S2 for a much more detailed geological map of the region.

program of gravity measurements to see if there is a gravity anomaly that would reflect a large buried crater. And fourth, we search for coarse proximal ejecta with shocked quartz, as evidence for an impact site under the basalts of the plateau.

In addition to the methods, data, and analyses presented in the paper associated with these 4 approaches, we provide additional supporting material for all 4 approaches in both an *SI Appendix* and in a data repository (25).

Presence of a Weathered Basaltic Component in the Tektites. Previous investigators have observed Mg concentrations in Australasian tektites higher than are typical in siliciclastic sediments (9, 14, 29) and have proposed a mafic component within the target rocks (14, 29). Sporadic enrichment in Ni, Co, and Cr (29–31), without a concomitant enrichment of highly siderophile elements (32), also points to a mafic terrestrial source (29, 32).

To examine further the possible presence of mafic rocks at the impact site at the time of impact, we performed a principal component analysis (PCA) on published (13) major-element compositions of 241 tektites from various locations. We found that >90% of the observed chemical variation can be readily explained by mixing of Mesozoic sequences of the Khorat Plateau with Bolaven basalts (Fig. 3 and *SI Appendix*, Figs. S4–S6), with more distal tektites, such as Australites, tending toward higher proportions of basalt.

Variations in the Sr-isotopic composition of Australasian tektites also show mixing of a low-Sr, high-$^{87/86}$Sr end member with a high-Sr, less-radiogenic component (33), again consistent with an admixture of Mesozoic bedrock with Bolaven volcanics and their weathering derivatives (*SI Appendix*, Fig. S7). Similarly, the more basaltlike Sr component is expressed to a greater extent in more distal tektites, the Australites in particular.

Characteristically high ^{10}Be in Australasian tektites is also noteworthy because it places considerable constraint on their genesis (13). Elevated ^{10}Be, a cosmogenic nuclide, implies that the impacted rocks contained a significant fraction of materials exposed to near-surface conditions within the few million years prior to the impact ($t_{1/2} = 1.39 \times 10^6$ y) (*SI Appendix*, Fig. S8).

We observe that basalts on the plateau weather largely to clay-rich saprolite within a couple of hundred thousand years (*SI Appendix*, Fig. S9). These clayey layers are well-suited for absorption and retention of meteoric ^{10}Be (34), which, unlike ^{10}Be produced in minerals and commonly used in determination of surface-exposure ages, forms by spallation of nitrogen and oxygen in the atmosphere and precipitates onto and into surface layers. Stacking of successive basalt flows would create a sequence of ^{10}Be-enriched saprolites many times thicker than what could be achieved on the erosional surface cut into the Mesozoic sandstones of the Bolaven Plateau. Thus, we propose that a stack of weathered preimpact basalt flows accounts for the anomalously high ^{10}Be concentrations observed in Australasian tektites. As with the geochemical trends described above, the increasing enrichment of ^{10}Be with distance from Indochina (13) is consistent with ejection trajectories that yield

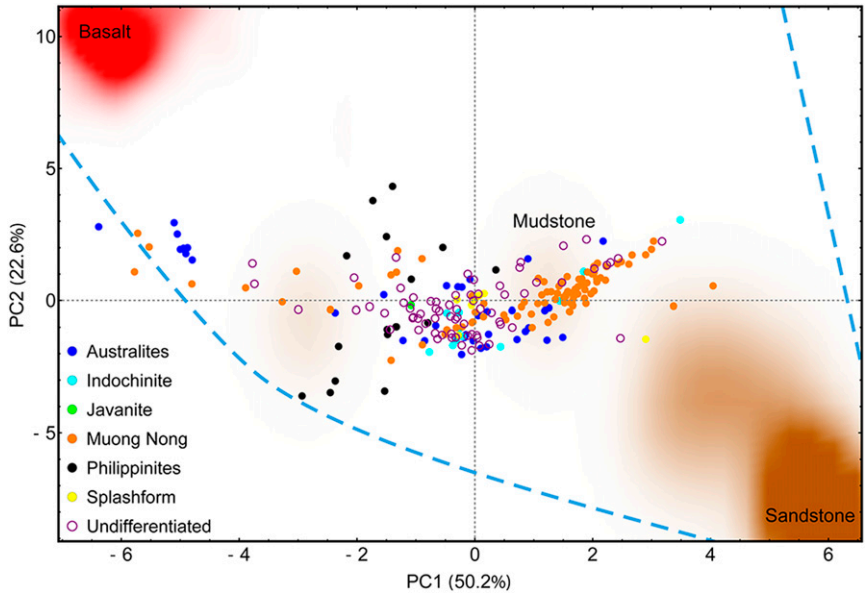

Fig. 3. PCA shows that 94% of tektite chemical variation can result from admixtures of Mesozoic bedrock and Bolaven Plateau basalt and their weathered derivatives. Blue dashed lines delineate the field of possible mixtures of Bolaven volcanics and Mesozoic bedrock. Principal components 1 and 2 alone explain 73% of the variation. The PCA analysis uses concentrations of 7 major-element oxides (SiO_2, Al_2O_3, TiO_2, FeO, MgO, CaO, K_2O) from 241 Australasian tektite samples. Tektites nearest the impact site (Muong Nong type) tend to plot closer to local Mesozoic strata. Distal tektites (Australites) tend to plot closer to basalts, but nearly all samples plot in between these end members. Tektite compositional data compiled from various sources, and variable loadings may be found in *SI Appendix* (25).

a greater basaltic component farther from the impact (*SI Appendix*, Fig. S8).

Ages of Exposed Basalts in the Summit Region. The law of superposition dictates that if lavas bury the impact crater, they must be younger than the impact. Conversely, if there is a component of basalt in the tektites, there must also be flows there that antedate it. Radioisotopic dating of flows on the plateau offers a test whether both of these 2 requirements are met.

Three published ^{40}Ar-^{39}Ar dates for the Bolaven lavas, ranging from 16 Ma to ∼50 ka, span the impact date (Fig. 2) (35). However, these dates are too few and too far from the proposed impact site to test either hypothesis.

The youthful appearance of the volcanic landforms in the vicinity of the summit and down most of the northern and southern flanks of the plateau suggests that most exposed flows are Late Quaternary in age. Most of the exposed flows and cinder cones of the Bolaven field do not exhibit appreciable erosion, despite the region's heavy (∼1.5 m/y) tropical rainfall [GMPC Precipitation Normals in mm/y, https://www.dwd.de/EN/ourservices/gpcc/gpcc.html, (2015)]. Canyons erode into only restricted, steep portions of the western and southern flanks of the field. Moreover, large tracts of the northern and southern field sport very thin tropical soils and exhibit scant saprolitization (*SI Appendix*, Fig. S9).

We dated 37 exposed flows via ^{40}Ar-^{39}Ar incremental-heating experiments. Our dating strategy was 2-pronged: We targeted a suite of lavas that spans the spectrum of geomorphologically young to old flows—that is, from those that exhibit little to no erosion or soil formation to those that are highly dissected and saprolitized and lack preserved upper-flow surfaces. We also focused on flows near the summit region, at and adjacent to the proposed epicenter of the impact. All analyses are of groundmass, so the ^{40}Ar-^{39}Ar dates reflect the time since cooling of the flows. None of the lavas contain significant excess Ar and all of the samples have isochrons with atmospheric intercepts. Sample location and related data are in *SI Appendix*, Table S1 and Basalt Information_Dataset S2, Ar-Ar Metadata_Dataset S3, and Basalt Geochemical Data_Dataset S4 (25).

The dates show that eruptions occurred over a sustained period of time—from ∼16 Ma to ∼27 ka. Fourteen samples antedate the impact, 21 postdate it, and 2 are contemporaneous with the impact, within error.

All 12 dates from lavas in the summit region and directly above the proposed crater are distinctly younger than the date of the impact (Figs. 2 and 4). Moreover, all but 2 of the dated flows within 8 km of the hypothetical crater perimeter are younger than or within error of the date of the impact, ranging from ∼51 to ∼779 ka. The two exceptions are these:

i) An ∼1.26-Ma date about 7 km west of the inferred crater rim and buried about 55 m below a nearby surface flow with a date indistinguishable from the 0.79-Ma date of the impact.

ii) An ∼12-Ma date from a 200-m-wide mound of highly weathered basalt about 6 km southeast of the inferred crater rim. This volcanic lump may be the remnant of a small scoria cone serendipitously left uncovered by the ejecta blanket and postimpact lavas.

The fact that all of the dates from lava flows above the proposed crater and most dates nearby are younger than the impact lends support to the hypothesis that Bolaven lavas fill the impact crater and completely obscure it. Conversely, preimpact ages for many flows on the periphery of the volcanic field, such as the 2 listed above, imply that there are basaltic lavas, now buried beneath the young summit lavas that were impacted by the bolide, as reflected especially in the chemistry of the more distal tektites.

Gravity Field of the Plateau. If there were a large crater buried beneath the summit region of the Bolaven Plateau, it would likely be apparent in the local gravity field. For example, if dense basalt fills the portion of the crater that is below the plane of the eroded bedrock surface, then it would manifest in a positive Bouguer gravity anomaly consistent with its horizontal dimensions. Alternatively, if loose impact debris fills this lower part of the crater, the gravity field would exhibit a

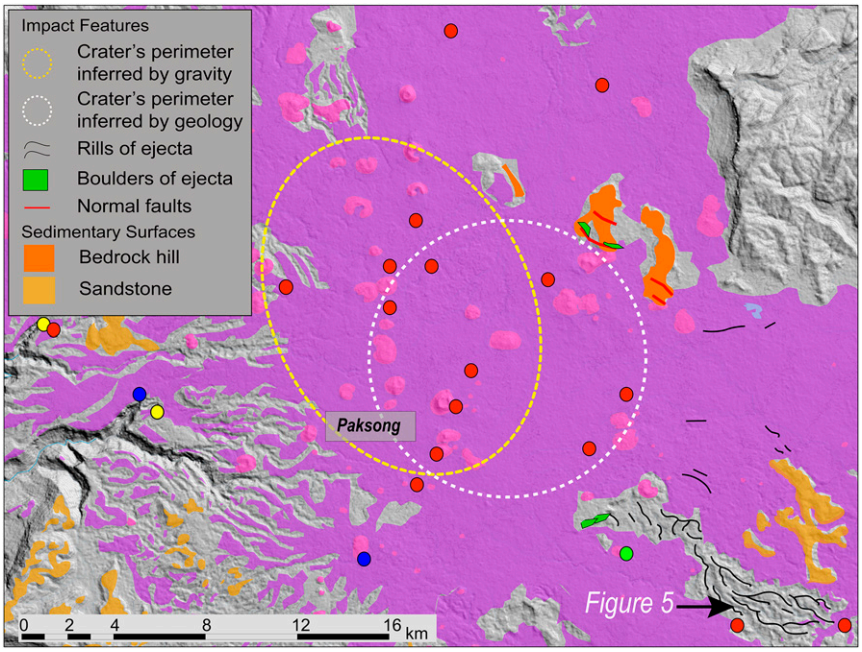

Fig. 4. Geological map of the summit region of the volcanic field. Dashed yellow ellipse marks the buried crater perimeter for the best-fitting gravity model. Dashed white circle marks the buried perimeter that best fits geological observations, which include proximity to normal faults, bedrock outcrops, and the proximal ejecta. Note that all but 2 ^{40}Ar-^{39}Ar ages within ~8 km of the inferred craters are younger than or within error of the 0.79-Ma age of the impact. Color-coded circles for dates are the same as in Fig. 2.

negative anomaly. If this part of the crater fill is a combination of basalt and impact debris, then the sign of the anomaly would depend on which of the deposits were prevalent. The presence of an ejecta blanket, perhaps 100 or 200 meters thick at the crater rim and lying atop the preimpact surface, should manifest as a negative anomaly.

In search of such an anomaly, we measured gravity at 404 locations, focused upon the summit region of the volcanic field but extending well beyond the Bolaven Plateau's perimeter, to constrain the regional gravity signal. The Bouguer gravity map obtained exhibits a regional southwest-to-northeast negative gradient ornamented with several smaller anomalies on the plateau (*SI Appendix*, Fig. S11*A*). These can only be evaluated after the additional processing that we describe below.

Of particular interest is a 20-km-wide, ~8-mGal anomaly in the summit region of the volcanic field. We processed the Bouguer gravity field to account for contributions from basalt flows (*SI Appendix*, Fig. S11*B*) and low-density components in the western-canyon fill and northern fan (*SI Appendix*, Fig. S11*C*) to yield the gravity field of *SI Appendix*, Fig. S11*D*, in which a large negative anomaly still remains within the region of the suspected impact crater.

Most of that remaining negative 6-mGal anomaly disappears if we replace a portion of the basalt by a 100-m-thick, elliptical lens of low-density breccia within an elongated crater that is about 13 km wide and 17 km long (*SI Appendix*, Fig. S11*E*). An ellipticity of around 30% would correspond to an impact angle of ~10° (36) after ref. 37. Of course, the use of this simple lens of low-density material would be a simplification of the actual geometry of materials related to the proposed crater. *SI Appendix*, Fig. S11 *F* and *G* show modeling of a more realistic cross-section through the impact crater.

The gravity anomaly cannot reflect the presence of a volcanic caldera, buried beneath the lavas, because calderas are features associated with large crustal magma reservoirs beneath composite volcanoes. The Bolaven field and similar intraplate volcanic fields comprise scattered, low-eruption-volume scoria cones and flows that reflect the rise of individual batches of magma (38, 39). The absence of long-lived, localized composite volcanoes on the Bolaven Plateau implies the absence of an underlying crustal magma reservoir (39). Thus, the presence of large crustal magma volumes characteristic of calderas is unlikely (40, 41). Further evidence against the existence of a buried caldera is the lack of Quaternary-Age ignimbrite or high-porosity volcanoclastic deposits (41) in the region of the Bolaven Plateau. These are commonly associated with composite volcanoes and calderas (42).

Another unlikely explanation for the gravity anomaly is a maar, a common feature of volcanic fields, characterized by craters with floors lying 5 to 400 m below the preeruptive surface, surrounded by a ring of ejecta and sourced from a low-density diatreme (43, 44). Maar craters are, however, only ~1 km in diameter (43), considerably smaller than the dimensions of the anomaly we observe.

Proximal Ejecta and Shocked Quartz. A fourth positive, and perhaps definitive test of the Bolaven crater hypothesis would be discovery of proximal ejecta. Lavas mantle most of the western half of the Bolaven Plateau, however, so one might consider the search for an ejecta blanket to be a fool's errand. Of great significance, then, is one small pie-shaped piece of oddly rilled terrain 10–20 km southeast of the summit of the volcanic field. This patch is the largest area near the summit that has escaped volcanic burial (Fig. 4 and *SI Appendix*, Fig. S2). Streams there flow southeastward in 40- to 50-m-deep valleys, away from the summit and with much closer spacing than drainages either atop or cutting into the lavas. In the 2 places where we could gain access through the thick jungle vegetation, the streambeds are flowing on in situ, flat-lying sandstone bedrock. This suggests that the rills have cut through a loose, 40- to 50-m-thick deposit to its basal contact with bedrock.

The looser material that forms the closely spaced rills is exposed in 2 road cuts. The better-exposed of these displays well a fining-upward breccia of angular sandstone and mudstone clasts (Fig. 5*A* and *SI Appendix*, Fig. S13). The lowest bed in the exposure is a monolithologic, cobbly, and bouldery fine-sandstone breccia, in a matrix of angular sand grains and pebbles. The overlying bed is a monolithologic, cobbly, boulder mudstone breccia. These 2 breccia

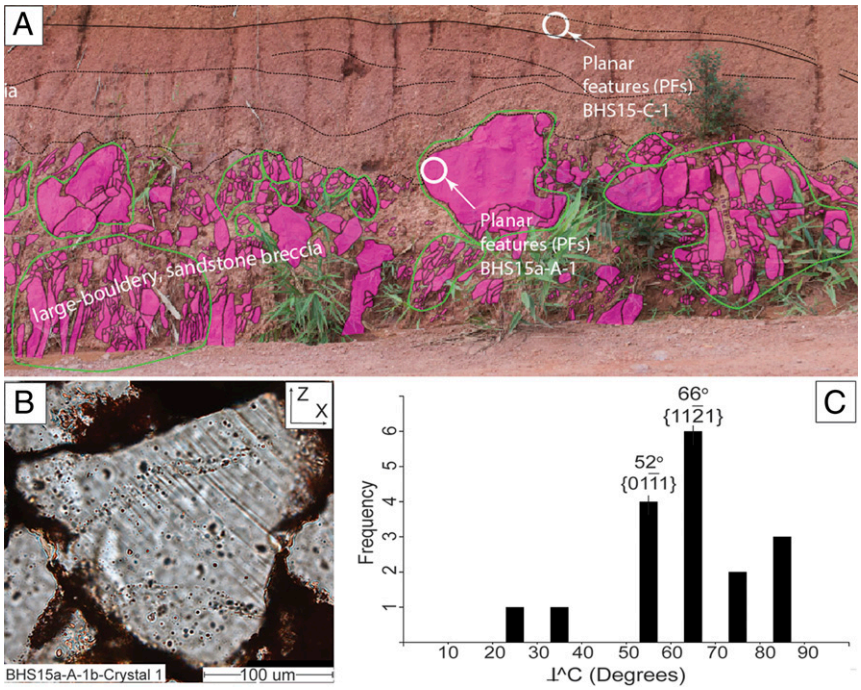

Fig. 5. Sandstone boulders within an impact-breccia deposit ~20 km southeast of the center of the proposed crater contains abundant planar fractures in quartz crystals. (*A*) Boulders shattered in situ at the end of ballistic trajectories from the proposed crater. See Fig. 4 for location of outcrop. (*B*) Microphotograph in plane-polarized light of parallel planar fractures (upper left to lower right) in 1 quartz crystal. The fractures are well-defined and do not cross grain boundaries. (*C*) Histogram of orientations of planar fractures in the quartz crystals shows the frequency distribution of the apparent angle between the quartz *c* axis and the pole to the planar fractures.

beds are remarkable for the fact that large domains within the outcrop comprise cobbles and boulders that fit together like jigsaw-puzzle pieces. Overlying the mudstone breccia is a thin sandstone breccia. Overlying and in sharp contact with this is a massive coarse silt to very fine sand, which we ascribe to deposition as a loesslike bed from a convecting cloud produced by the impact, similar to the genesis proposed for deposits in eastern Thailand (16).

The sedimentological and stratigraphic nature of the lower 3 beds in this outcrop is consistent with the rapid accumulation of clasts at the end of ballistic trajectories from the impact crater. The angular nature of both framework and matrix indicates that they did not experience rounding during transport, as would be expected if they arrived as bedload in a very powerful stream. The jigsaw-puzzle–like fitting of neighboring clasts in the coarse, lower 2 beds is wholly unlike outcrops of intensely weathered siliclastic bedrock elsewhere on the plateau. These jigsaw patterns imply that the boulders shattered at the site and support the argument that they could not have been transported to the site in a debris flow or weathered in situ. Moreover, the size of the sandstone boulders implies very high energies of emplacement, far greater than are plausible in the small neighboring stream, which has no large tributaries and descends only about 100 m from its headwaters 4 km upstream.

We argue that this outcrop exposes part of the ejecta blanket that surrounds the impact site. The fact that the thick mudstone breccia overlies the sandstone breccia supports this claim, because inversion of the ordering of the Mesozoic stratigraphy of the plateau—roughly 200 m of sandstone overlying about 250 m of mudstone—is what one would expect in the ejecta blanket (37, 45). We estimate the impact velocity for these boulders to be about 450 m/s, assuming that they exited the crater at an angle between 45° and 60° (*SI Appendix*, Fig. S13 and associated text). If these beds represent inverted stratigraphy of the target rocks, one would expect a breccia bed comprising basalt debris directly beneath the sandstone breccia layer and atop bedrock. Unfortunately, the several meters of section between the sandstone bed and bedrock is not exposed, but there are rare, loose basalt clasts atop bedrock in a nearby streambed that might have come from that unexposed, basal part of the breccia.

Discovery of shocked quartz within the sandstone boulders would provide an independent test of whether this outcrop represents a part of the eject blanket (46). Not finding evidence of shocked quartz would support the argument that this is not an impact deposit, even though its sedimentological nature and setting preclude any other origin that we can imagine. Petrographic examination reveals that the quartz grains in the sandstone boulders do indeed have planar fractures like those caused by high-velocity impacts, but quartz grains in the underlying bedrock do not.

First we examine differences in the petrographic textures of the in situ bedrock and the overlying ejecta deposit. *SI Appendix*, Fig. S14 displays images of the 2 rocks, side by side. Note that the bedrock comprises dominantly angular to subangular medium-size grains of quartz sand with little to no matrix. In contrast the boulder from the ejecta deposit consists principally of very fine to fine-grained angular quartz sand floating in a nondescript, clayey matrix. We are uncertain whether this texture is an original depositional texture or the result of postdepositional comminution and weathering, but the latter is a possibility.

Fractures appear in the quartz grains of both the bedrock and the boulders. However, fractures in the bedrock grains do not have the characteristics of shock-related fractures: They are curved and display variations in thickness (*SI Appendix*, Fig. S14 *A* and *B*). They are not evenly distributed within a grain and in some cases continue across grain boundaries. Similar fractures exist in some grains of the sandstone boulders (*SI Appendix*, Fig. S14*E*).

However, we also observe grains in the boulders that display very distinct, parallel, planar fractures about 2 μm wide and 2–18 μm apart (Fig. 5*B* and *SI Appendix*, Fig. S14*D*). These do not cross grain boundaries.

In some of these crystals we measured the apparent polar angles between the index plane of the planar fractures and the c axes of the host quartz grains, to see if they are within the range of crystallographic orientations proposed by others (47) to be typical of shock-related features. Fig. 5*C* and *SI Appendix*, Table S2 show that most of the calculated polar angles cluster around 52° and 66°, which could correspond to Miller Index planes, notably $\{10\bar{1}1\}$, that are typical in shocked quartz grains. Others (46, 48) have used the predominance of fractures with these crystallographic orientations to distinguish high-pressure (10–35 GPa) planar deformation features (PDFs). Compelling evidence that ours are PDFs would require measurement of 100 or so samples (49). We have elected not to do such a comprehensive test here, since we have so many other lines of evidence that the deposit is part of a proximal ejecta blanket—i.e., the poorly sorted nature of the deposit itself, the angularity of both its large and small clasts, and the proximity of the deposit to the proposed crater rim. We hypothesize that these quartz grains do indeed reflect the weak (<10–20 GPa) shocking that one would expect in rocks that originated near the perimeter of the excavating crater (37, 50, 51).

One other site that might contain proximal ejecta is on the northeast flank of the suspected crater. Strewn on a small, faulted inselberg of Mesozoic bedrock surrounded by basalt (Fig. 4 and *SI Appendix*, Fig. S2) are large blocks of cross-bedded Mesozoic fluvial sandstone (*SI Appendix*, Fig. S16). None of these large boulder slabs are overturned, but the extreme discordance of dips and strikes from boulder to boulder is consistent with their having been thrown out of the crater onto the crater rim. Alternatively, these loose blocks might have been dislodged by the passage of impact shock waves or normal faulting underfoot during collapse of the impact crater rim. Similar outcrops of very large boulders occur on the crest of a ridge 1 or 2 km southeast of the proposed crater rim.

Data Availability. Supplementary datasets are in the public data repository hosted by Nanyang Technological University (DR-NTU). The data package is entitled Supplementary data for "Australasian Impact Crater Buried under the Bolaven Volcanic Field, *Southern* Laos" (https://doi.org/10.21979/N9/CTNDZQ) (25).

The dataset contains these files: Tektite Information_Dataset S1. The table contains information about our collection of tektites, including measurements of weight and size and an estimation of the difference in elevation of the sample location with respect to the Mekong River system; Basalt Information_Dataset S2. The table contains general information of our collection of basalt specimens; Ar-Ar Metadata_Dataset S3. This contains a table with all of the argon isotope data as well as the plateaux of the dated samples. These data will allow for independent data assessment and future reevaluations or recalculations of ages; Basalt Geochemical Data_Dataset S4. Report of geochemical analysis performed at Actlabs; Geologic Map_Dataset S5. Illustrator file of a detailed geologic map of the Bolaven Plateau; and Breccia Outcrop_Dataset S6. Illustrator file comprising high-resolution photographs of the breccia deposit and our detailed interpretation.

Conclusion

Four lines of evidence imply strongly that the impact that produced the vast Australasian strewn field lies beneath young lavas of the Bolaven volcanic field in Southern Laos. First, the Mesozoic siliclastic rocks and young overlying preimpact basalts of the plateau are consistent with tektite geochemistry and relict mineralogy. Second, exposed lava flows above and near the hypothesized crater are younger than the 0.79-Ma date of the impact. Third, a negative gravity anomaly at the summit region of the volcanic field is of a dimension and magnitude consistent with the presence of low-density clastic deposits associated with an impact crater. Finally, an outcrop 10–20 km from the proposed impact site consists of brecciated sandstone and mudstone boulders that appear to have shattered in situ during ballistic emplacement. PDFs in quartz grains within 1 of the boulders imply shock metamorphism that supports this interpretation.

ACKNOWLEDGMENTS. This work was funded primarily by the Earth Observatory of Singapore, which receives most of its funding from the National Research Foundation Singapore and the Singapore Ministry of Education under the Research Centers of Excellence initiative. We acknowledge and appreciate the participation and generosity of the Department of Mineral Resources and Environment, Thailand, the Department of Geology and Mines, Lao PDR, and the Facility for Analysis, Characterisation, Testing, and Simulation at Nanyang Technological University. We are grateful to Jeff Oalmann, Aaron Satkoski, and Jingxian Wang for their assistance with this work, as well as Paul Tapponnier and Michael Zolensky for insightful discussions.

1. W. H. Schwarz *et al.*, Coeval ages of Australasian, Central American and Western Canadian tektites reveal multiple impacts 790 ka ago. *Geochim. Cosmochim. Acta* **178**, 307–319 (2016).
2. G. Izett, J. Obradovich, Laser-fusion 40Ar/39 age of Australasian tektites. *Lunar Planet. Sci. Conf.* **23**, 593–594 (1992).
3. B. P. Glass, J. E. Pizzuto, Geographic variation in Australasian microtektite concentrations: Implications concerning the location and size of the source crater. *J. Geophys. Res.* **99**, 19075–19081 (1994).
4. R. J. Ford, An empirical-model for the Australasian tektite field. *Aust. J. Earth Sci.* **35**, 483–490 (1988).
5. L. Folco *et al.*, Shocked quartz and other mineral inclusions in Australasian microtektites. *Geology* **38**, 211–214 (2010).
6. B. P. Glass, C. Koeberl, Australasian microtektites and associated impact ejecta in the South China Sea and the Middle Pleistocene supereruption of Toba. *Meteorit. Planet. Sci.* **41**, 305–326 (2006).
7. M. Y. Lee, K. Y. Wei, Australasian microtektites in the South China Sea and the West Philippine Sea: Implications for age, size, and location of the impact crater. *Meteorit. Planet. Sci.* **35**, 1151–1155 (2000).
8. B. P. Glass, M. Fries, Micro-Raman spectroscopic study of fine-grained, shock-metamorphosed rock fragments from the Australasian microtektite layer. *Meteorit. Planet. Sci.* **43**, 1487–1496 (2008).
9. K. Amare, C. Koeberl, Variation of chemical composition in Australasian tektites from different localities in Vietnam. *Meteorit. Planet. Sci.* **41**, 107–123 (2006).
10. B. P. Glass, R. A. Barlow, Mineral inclusions in Muong Nong-type Indochinites: Implications for concerning parent material and process of formation. *Meteoritics* **14**, 55–67 (1979).
11. J. D. Blum, D. A. Papanastassiou, C. Koeberl, G. J. Wasserburg, Neodymium and strontium isotopic study of Australasian tektites–New constraints on the provenance and age of target materials. *Geochim. Cosmochim. Acta* **56**, 483–492 (1992).
12. M. S. Prasad, V. P. Mahale, V. N. Kodagali, New sites of Australasian microtektites in the central Indian Ocean: Implications for the location and size of source crater. *J. Geophys. Res.* **112**, E06007 (2007).
13. P. Ma *et al.*, Beryllium-10 in Australasian tektites: Constraints on the location of the source crater. *Geochim. Cosmochim. Acta* **68**, 3883–3896 (2004).
14. C. Koeberl, Geochemistry and origin of Muong Nong-type tektites. *Geochim. Cosmochim. Acta* **56**, 1033–1064 (1992).
15. V. E. Barnes, K. Pitakpaivan, Origin of indochinites tektites. *Proc. Natl. Acad. Sci. U.S.A.* **48**, 947–955 (1962).
16. S. Bunopas *et al.*, "Early Quaternary global terrestrial impact of a whole comet in the Australasian tektite field, newest apparent evidences discovery from Thailand and East Asia" in *Proceedings, Bulletin of the Geological Society of Malaysia 45 Ninth Regional Congress on Geology, Mineral and Energy Resources of Southeast Asia–GEOSEA '98* (Geological Society of Malaysia, 1998), pp. 555–575.
17. J. Hartung, C. Koeberl, In search of the Australasian tektite source crater: The Tonle Sap hypothesis. *Meteoritics* **29**, 411–416 (1994).
18. J. Mizera, Z. Řanda, J. Kameník, On a possible parent crater for Australasian tektites: Geochemical, isotopic, geographical and other constraints. *Earth Sci. Rev.* **154**, 123–137 (2016).
19. C. Schnetzler, J. McHone, Source of Australasian tektites: Investigating possible impact sites in Laos. *Meteorit. Planet. Sci.* **31**, 73–76 (1996).
20. A. Whymark, "Review of the Australasian Tektite Source Crater Location and Candidate Structure in the Song Hong-Yinggehai Basin, Gulf of Tonkin" in *44th Lunar and Planetary Science Conference* (2013), LPI. Contribution No. 1719, p. 1077. https://ui.adsabs.harvard.edu/#abs/2013LPI....44.1077W/abstract. Accessed 13 December 2019.
21. A. J. Cavosie, N. E. Timms, T. M. Erickson, C. Koeberl, New clues from Earth's most elusive impact crater: Evidence of reidite in Australasian tektites from Thailand. *Geology*, **46**, 203–206 (2017).
22. J. T. Wasson, "An origin of splash-form tektites in impact plumes" in *4th Lunar and Planetary Science Conference* (2015), pp. 2879. https://www.hou.usra.edu/meetings/lpsc2015/pdf/2879.pdf. Accessed 13 December 2019.

23. J. T. Wasson, K. Mezger, "Isotopic evidence of tektite formation from loess" in *70th Annual Meteoritical Society Meeting* (Meteoritics and Planetary Science Supplement, 2007).
24. H. J. Melosh, *Impact Cratering: A Geologic Process* (Oxford University Press, 1996).
25. D. A. Schonwalder Angel, K. Sieh, J. Herrin, Supplementary data for "Australasian Impact Crater Buried under the Bolaven Volcanic Field, Southern Laos." Dataverse DR-NTU (Data). https://researchdata.ntu.edu.sg/dataset.xhtml?persistentId=doi:10.21979/N9/CTNDZQ. Deposited 22 February 2019.
26. J. Hartung, A. Rivolo, A possible source in Cambodia for Australasian tektites. *Meteoritics* **14**, 153–160 (1979).
27. T. Kenkmann, R. V. Maier, S. Sturm, M.-H. Zhu, "A new tektite discovery in the Guangdong Province, China, and the search for the source crater of the Australasian tektite strewn field" in *77th Annual Meteoritical Society Meeting* (2014), LPI Contributions 1800, 5322. https://www.hou.usra.edu/meetings/metsoc2014/pdf/5322.pdf. Accessed 13 December 2019.
28. Anonymous, Geological Map of Asia, 1:500,000 (Academy of Geological Sciences of China, Beijing, 1975).
29. J. T. Wasson, Layered tektites: A multiple impact origin for the Australasian tektites. *Earth Planet. Sci. Lett.* **102**, 95–109 (1991).
30. S. Goderis, R. Tagle, J. Fritz, R. Bartoschewitz, N. Artemieva, On the nature of the Ni-rich component in splash-form Australasian tektites. *Geochim. Cosmochim. Acta* **217**, 28–50 (2017).
31. L. Folco, B. P. Glass, M. D'Orazio, P. Rochette, Australasian microtektites: Impactor identification using Cr, Co and Ni ratios. *Geochim. Cosmochim. Acta* **222**, 550–568 (2018).
32. N. Shirai, R. Akhter, M. Ebihara, "Precursor materials of Australasian tektites in light of chemical compositions" in *47th Lunar and Planetary Science Conference, March 21-25* (2016), LPI Contribution No. 1903, p. 1847. https://ui.adsabs.harvard.edu/#abs/2016LPI....47.1847S/abstract. Accessed 13 December 2019.
33. J. D. Blum, D. A. Papanastassiou, C. Koeberl, G. J. Wasserburg, Neodymium and strontium isotopic study of Australasian tektites: New constraints on the provenance and age of target materials. *Geochim. Cosmochim. Acta* **56**, 483–492 (1992)
34. K. Maher, F. von Blanckenburg, Surface ages and weathering rates from 10Be (meteoric) and 10Be/9Be: Insights from differential mass balance and reactive transport modeling. *Chem. Geol.* **446**, 70–86 (2016).
35. K. Sanematsu, T. Moriyama, S. Laochou, Y. Watanabe, Laterization of basalts and sandstone associated with the enrichment of Al, Ga and Sc in the Bolaven Plateau, southern Laos. *Bull. Geol. Surv. Jpn.* **62**, 105–129 (2011)
36. D. Gault, J. Wedekind, "Experimental studies of oblique impact" in *9th Lunar and Planetary Science Conference* (Pergamon Press, Houston, TX, 1978), pp. 3843–3875.
37. H. J. Melosh, *Impact Cratering: A Geologic Process* (Oxford University Press, 1989).
38. L. McGee, C. Beter, I. Smith, S. Turner, Dynamics of melting beneath a small-scale basaltic system: A U-Th-Ra study from Rangitoto volcano, Auckland volcanic field, New Zealand. *Contrib. Mineral. Petrol.* **162**, 547–563 (2011).
39. G. Valentine, N. Hirano, Mechanisms of low-flux intraplate volcanic fields–Basin and Range (North America) and northwest Pacific Ocean. *Geology* **38**, 55–58 (2010).
40. A. Gudmundsson, Magma chambers: Formation, local stresses, excess pressures, and compartments. *J. Volcanol. Geotherm. Res.* **237-238**, 19–41 (2012).
41. B. Kennedy *et al*., Magma plumbing beneath collapse caldera volcanic systems. *Earth Sci. Rev.* **177**, 404–424 (2018).
42. K. V. Cashman, G. Giordano, Calderas and magma reservoirs. *J. Volcanol. Geotherm. Res.* **288**, 28–45 (2014).
43. A. Graettinger, Trends in maar crater size and shape using the global Maar Volcano Location and Shape (MaarVLS) database. *J. Volcanol. Geotherm. Res.* **357**, 1–13 (2018).
44. J. White, P. Ross, Maar-diatreme volcanoes: A review. *J. Volcanol. Geotherm. Res.* **201**, 1–29 (2011).
45. E. M. Shoemaker, "Impact mechanics at meteor crater, Arizona" in *The Moon, Meteorites and Comets*, B. M. Middlehurts, G. P. Kuiper, Eds. (University of Chicago Press, London, 1963), vol. 4, pp 301–336.
46. B. M. French, C. Koeberl, The convincing identification of terrestrial meteorite impact structures: What works, what doesn't, and why. *Earth Sci. Rev.* **98**, 123–170 (2010).
47. D. Stöffler, F. Langenhorst, Shock metamorphism of quartz in nature and experiment: I. Basic observation and theory. *Meteoritics* **29**, 155–181 (1994).
48. R. Langenhorst, A. Deutsch, Shock metamorphism of minerals. *Elements* **8**, 31–36 (2012).
49. L. Ferriere, J. Morrow, T. Amgaa, C. Koeberl, Systematic study of universal-stage measurements of planar deformation features in shocked quartz: Implications for statistical significance and representation of results. *Meteorit. Planet. Sci.* **44**, 925–940 (2009).
50. B. French, The importance of being cratered: The new role of meteorite impact as a normal geological process. *Meteorit. Planet. Sci.* **39**, 169–197 (2004).
51. S. Kieffer, P. Phakey, J. Christie, Shock processes in porous quartzite: Transmission electron microscope observations and theory. *Contrib. Mineral. Petrol.* **59**, 41–93 (1976).
52. P. S. Fiske *et al*., Layered tektites of southeast Asia: Field studies in central Laos and Vietnam. *Meteorit. Planet. Sci.* **34**, 757–761 (1999).
53. S. M. Barr, A. S. Macdonald, Geochemistry and geochronology of late Cenozoic basalts of southeast Asia. *Geol. Soc. Am. Bull.* **92**, 1069–1142 (1981)
54. J. L. Whitford-Stark, *A Survey of Cenozoic Volcanism on Mainland Asia* (Geological Society of America Special Papers, 1987), vol. 213, pp. 1–74, 10.1130/SPE1213-p1131.
55. J.-S. Ren *et al*., 1:5 million international geological map of Asia. *Acta Geoscientica Sinica* **34**, 24–30 (2013).
56. L. Folco, M. D'Orazio, M. Gemelli, P. Rochette, Stretching out the Australasian microtektite strewn field in Victoria Land Transantarctic Mountains. *Polar Sci.* **2**, 147–159 (2016).